Iranian Journal of Physics Research, Vol. 21, No. 3, 2021

Fabrication of a dye-based random laser using ZnS:Mn quantum dots and investigating the effects of their concentration

P Rafieipour, A Ghasempour Ardakani*, M Jaafar Samimipour, and J Tashkhourian
Department of Physics, College of Science, Shiraz University, Shiraz, Iran

E-mail: aghasempour@shirazu.ac.ir

(Received 19 August 2020 ; in final form 15 December 2020)

Abstract
Zinc chalcogenide quantum dots (QDs) doped with paramagnetic transition metal ions (particularly ZnS:Mn QDs) are new attractive but rarely examined semiconductor nanocrystals that have excellent optical properties and enhanced thermal and environmental stability compared to Cd-based QDs. In this paper, we demonstrate a dye-based random laser (RL) with nonresonant feedback using ZnS:Mn QDs as the scattering medium that are dispersed in a Rhodamine B (RhB) dye solution. The nonlinear variation of the emission spectrum as a function of the excitation energy implies a random lasing threshold. Moreover, we observe a blue-shift of the emission wavelength by 10.3 nm and a 5.3 times decrease in the RL threshold by increasing the scatterer concentration. We also provide a theoretical discussion based on the diffusion theory for explaining the observed experimental results.

Keywords: Mn doped ZnS quantum dots, multiple light scattering, random lasers

1. Introduction

Lasing action can be established in an optical gain medium without a Fabry-Perot resonator, by designing and introducing strongly scattering random elements into the gain medium. This encourages multiple scattering media such as dielectric, metal and magnetic nanoparticles as well as nano- and microstructures, resulting in the fabrication of many different kinds of randomness-based lasers or random lasers (RLs) [1-28]. Although the physical mechanism responsible for light amplification in RLs is the stimulated emission process, the optical feedback in RLs is based on light multi-scattering inside the random amplifying medium [29,30]. Since there is no need to align the mirrors with high precision and design resonators with high quality in the fabrication process, RLs are of considerable attention for developing many optoelectronic and laser-related technologies [31-34]. The interest in quantum dots-based random lasers (QDs-RLs) stems from their size dependent emission properties and potential applications in display devices, bioimaging systems, sensors and optical barcodes. So far, the red-emitting CdSe/ZnS core-shell colloidal QDs were a kind of popular semiconductor nanocrystals that can be found numerously in literature. For example, they have been used as the gain medium in a waveguide RL scheme based on the manually-written grooves on a glass substrate [35] and a polarization controllable RL provided by introducing ellipsoidal Ag nanoparticles as the scattering elements [36]. In another research [37], CdSe/ZnS core-shell colloidal QDs have been dispersed in an inhomogeneous polymeric matrix with random refractive index fluctuation and the corresponding RL spectral characteristics have been investigated as a function of the detection angle, excitation position and excitation area. Furthermore, CdSe/CdS colloidal QDs were another candidate as the gain and/or feedback part of a RL system [38]. In addition, mixing Rh6G dye solution with colloidal CdSe QDs has been shown to enhance the RL emission from CdSe QDs that were used as both of gain and scattering media [39]. In another research [40], CdS nanoparticles were also dissolved in an ethanol solution of 4- dicyanomethylene- 2- methyl- 6- p-dimethylaminostyryl -4H- pyran (DCM) dye and employed as the scattering elements for providing the optical feedback. Moreover, a dipole transition model was implemented for describing the spectral characteristics and angular dependences of lasing modes and the output intensity [40].

Although Cd-based II-VI QDs are among the few marvelous semiconductor nanocrystals that have been

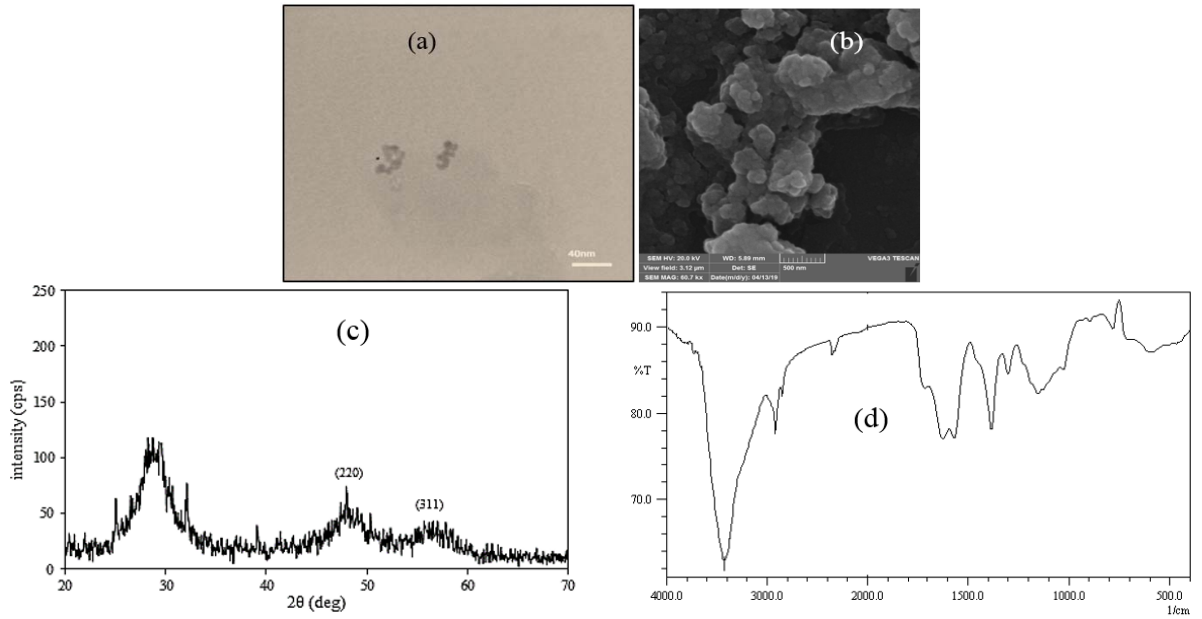

Fig. 1. (a) TEM image - scale bar is 40 nm, (b) SEM image - scale bar is 500 nm, (c) XRD and (d) FT-IR spectra of ZnS:Mn QDs powder.

the main subject of the studies on QDs-RLs, they suffer from inherent toxicity which limits their usage in practical applications such as bioimaging systems and sensors. To date, much less attention has been paid for RLs fabricated based on Zinc chalcogenide QDs such as ZnS and ZnSe [41-43]. It is worth noting that these semiconductor nanocrystals doped with paramagnetic transition metal ions (especially Mn^{2+} ions) are potential alternatives to Cd-based QDs due to their lower toxicity, longer excited state lifetimes, larger Stokes shifts and enhanced thermal and environmental stability. These remarkable advantageous make them an excellent candidate for the gain or scattering part of the RL systems that are suitable for designing high performance bioimaging and optoelectronic devices. It is also worth mentioning that controlling the optical, electronic, spintronic and transport properties of ZnS QDs doped with Mn^{2+} ions (ZnS:Mn QDs) is possible by changing the concentration of Mn^{2+} ions [44-46]. Hence, in this paper, we suggest the use of ZnS:Mn QDs as the scattering medium that are dispersed in an ethylene glycol solution of rhodamine B (RhB) dye. By comparing the emission spectrum of the colloidal solution of RhB dye and ZnS:Mn QDs with that of neat dye solution, it is demonstrated that adding ZnS:Mn QDs into the gain medium increases the emission peak intensity and decreases the emission peak linewidth, significantly. In order to obtain the threshold pump energy at which the random lasing oscillation triggers, we measure the emission spectra corresponding to the colloidal solution of RhB dye and ZnS:Mn QDs at different values of the pump energy and investigate the pump energy dependences of the output intensity. Thereafter, we change the concentration of ZnS:Mn QDs and investigate the variation of the RL spectral characteristics as a function of the scatterer concentration. It is well-known as an experimental approach to validate the role of ZnS:Mn QDs (the scattering medium) in providing the necessary optical feedback for the RL emission. Obtained results are in agreement with the previous reports on RLs with a nonresonant feedback [47, 48].

The remaining parts of this paper are organized as follows: Section 2 describes the synthesis method along with the related structural characterization analysis. Also, the experimental set up used in the RL experiments is illustrated in section 2. Section 3 covers the results of the experiments and the related discussions. In section 4, we finish the paper with a brief conclusion.

2. Experimental method

2. 1. synthesis and characterization of ZnS:Mn QDs

The synthesis of ZnS:Mn QDs was performed according to [49]. Briefly, 5.0 mL of 0.1 mol L^{-1} $Zn(CH_3COO)_2$, 20.0 mL of 0.1 mol L^{-1} mercaptoacetic acid and 1.5 ml of 0.01 mol L^{-1} $Mn(CH_3COO)_2$ were added into a three-necked flask and diluted to 50.0 mL with doubly deionized water. The PH of the mixed solution was adjusted to be 10.5 using 2.0 mol L^{-1} NaOH. Then nitrogen gas was passed for 30 minutes at room temperature in order to remove oxygen. Then, 5.0 mL of 0.1 mol L^{-1} Na_2S was quickly injected into the solution under vigorous stirring and nitrogen atmosphere for approximately 15 min. Finally, the solution was aged to 50 °C for 2 hours in air. The aged solution was precipitated with anhydrous ethanol. After that, the precipitate was centrifuged and washed with ethanol and then dried in vacuum to obtain ZnS:Mn nanocrystals.

The morphological features and the diameter of ZnS:Mn QDs were characterized by fast Fourier transform infrared (FT-IR) spectroscopy, transmission electron microscope (TEM), scanning electron microscope (SEM) and X-ray diffraction (XRD) analysis. Fig. 1 (a) shows the TEM image of the nanocrystals after reflux. It is observed that ZnS:Mn QDs have spherical shape with nearly uniform size and diameter of 6.15 nm. The observed little agglomeration is due to the evaporation of the solvent. Also an SEM

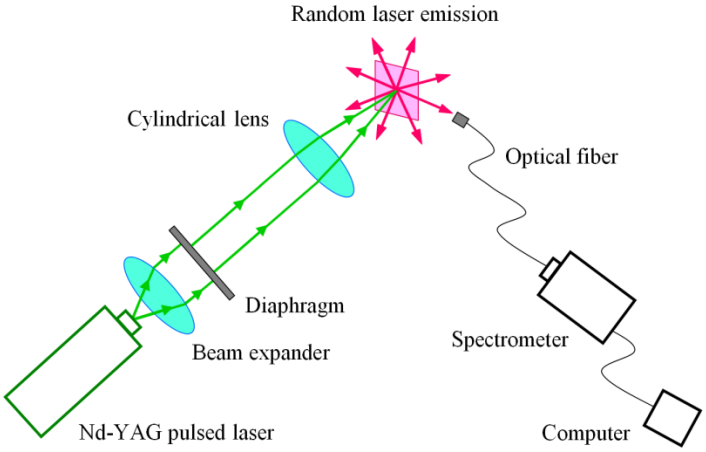

Fig. 2. A layout of the experimental set up.

image of ZnS:Mn QDs that are dispersed in the ethylene glycol solution of 10.44 mM RhB dye is presented in Fig. 1 (b). The scale bar is 500 nm. The larger units of the agglomerated ZnS:Mn QDs are clearly observed.

The XRD pattern of ZnS:Mn QDs which are obtained under 210 °C drying temperature, is shown in Fig. 1 (c). The XRD spectra of QDs showed no significant discrepancy for different 60 °C, 120 °C and 210 °C drying temperatures. The diffraction features appearing at 28.5°, 47.5° and 56.3° are very consistent with the values reported in the standard card (PDF–card 5–566) and correspond to the (111), (220) and (311) planes of cubic sphalerite ZnS, respectively. It implies that the ZnS:Mn QDs possess the cubic sphalerite ZnS crystal model. The averaged crystallite size (D) of ZnS:Mn QDs is estimated as 3.8 nm, according to Debye-Scherrer formula [49]:

$$D = \frac{k\lambda}{\beta \cos\theta} \quad (1)$$

Where D is the averaged crystallite size, λ is the wavelength of X-ray (the line kα of Cu with wavelength of 0.15406 nm), θ is the glancing angle between X-rays and a crystal face, k is a constant with the value of 0.89 and β is the full-width at half maximum (FWHM) of the diffraction line.

The FT-IR spectrum of ZnS:Mn QDs is shown in Fig. 1 (d). The peaks from left to right correspond to the stretching of O—H, C—H, C=O, CH_2, C—O and Zn—S bonds, respectively.

2. 2. RL experiments

The gain medium was a homogeneous solution of RhB dye (Aldrich) that was dissolved in ethylene glycol (Merck) with a concentration of 10.44 mM. As the scattering medium, ZnS:Mn QDs were dispersed in RhB dye solution with a concentration of 35 mg mL^{-1}. The mixed solution was first stirred, using a magnetic stirrer, for 90 minutes and then ultrasound for 30 minutes. Finally, the prepared colloidal solution was transferred into a cuvette for lasing experiments. In order to investigate the effects of the scatterer concentration on random lasing emission, we prepared other samples composed of different concentrations of ZnS:Mn QDs such as 5 mg mL^{-1}, 10 mg mL^{-1}, 15 mg mL^{-1}, 20 mg mL^{-1}, 25 mg mL^{-1}, 30 mg mL^{-1} and 40 mg mL^{-1} that were dispersed in 10.44 mM RhB dye solution. Also a sample composed of 10.44 mM RhB dye without ZnS:Mn QDs was prepared in the same way. It should be noted that the nanoparticle sedimentation was very probable using very high concentrations of ZnS:Mn QDs. Hence, the concentration of ZnS:Mn QDs could not exceed the amount of 40 mg mL^{-1} in our laboratory.

Figure 2 presents a schematic diagram of the experimental set up. The second harmonic of a neodymium doped yttrium aluminum garnet (Nd-YAG) laser with 532 nm wavelength, 10 ns pulse duration and repetition rate of 10 Hz illuminated the sample normally. By using a diaphragm and a cylindrical lens in front of the pump laser, we adjusted the excitation area on the sample as a stripe with 10.15 mm length and 1.45 mm width. The emitted light was collected by an optical fiber and coupled into a spectrometer (ocean optics) with the resolution of 0.5 nm. Then, a computer was used for recording the emission spectra of the pumped sample.

3. Results and discussions

We start with the measurement of the emission spectra corresponding to the sample composed of 10.44 mM RhB dye and 35 mg mL^{-1} ZnS:Mn QDs. The pump energy ranges from the low value 0.15 mJ/pulse to the high value 28.1 mJ/pulse. We then repeat this work for another sample composed of 10.44 mM RhB dye without ZnS:Mn QDs. The emission spectra corresponding to both samples are compared with each other in Fig. 3, for the constant pump energy 28.1 mJ/pulse. We observe two noticeable differences in their corresponding emission intensities and linewidths (FWHM). As it is shown in Fig. 3(a), a single emission peak with the central wavelength 603 nm is observed in the emission spectrum of the sample composed of 35 mg mL^{-1} ZnS:Mn QDs and 10.44 mM RhB dye. On the contrary, we observe that the emission spectrum of the sample composed of 10.44 mM RhB dye without ZnS:Mn QDs is very broad and weak, resembling the spontaneous emission spectrum of RhB dye molecules.

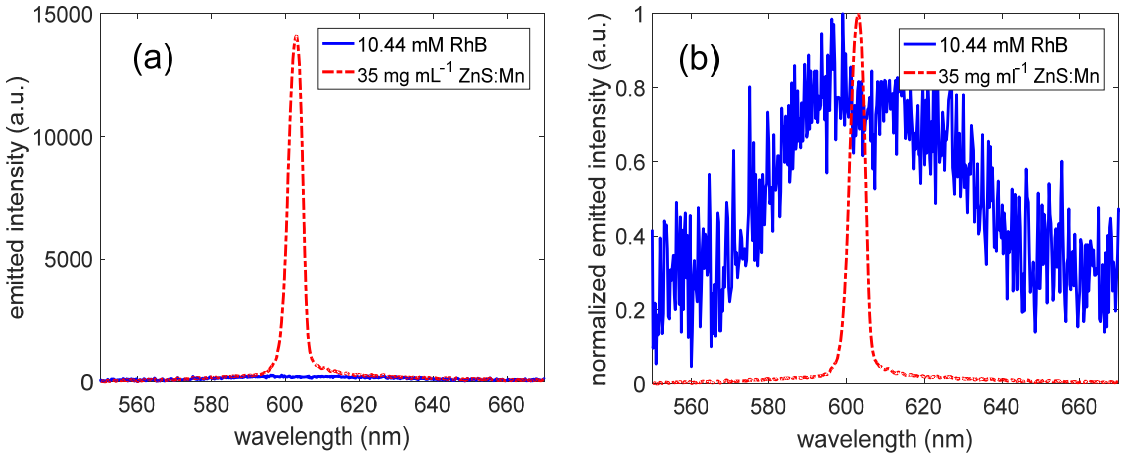

Fig. 3. (a) The emission spectra, and (b) the normalized emission spectra corresponding to the sample composed of 10.44 mM RhB dye without ZnS:Mn QDs and the sample composed of 10.44 mM RhB dye with 35 mg mL^{-1} ZnS:Mn QDs. The pump energy is 28.1 mJ/cm^2.

The maximum emitted intensity of the sample composed of 35 mg mL^{-1} ZnS:Mn QDs and 10.44 mM RhB dye is approximately 50 times higher than the maximum emitted intensity corresponding to the sample composed of the neat dye solution. Figure 3(b) shows the normalized emission spectra of these two samples at the same pump energy of 28.1 mJ/pulse. The linewidths of the emission spectra corresponding to these two samples are 4.5 nm and 65 nm, respectively. By comparing the normalized emission spectra of these two samples, it is clearly seen that the linewidth of the emission peak corresponding to the sample composed of 35 mg mL^{-1} ZnS:Mn QDs and 10.44 mM RhB dye is 14 times lower than the linewidth of the broadband emission spectrum corresponding to the neat dye solution.

We then come to this conclusion that introducing ZnS:Mn QDs in the gain medium affects the emission spectrum, significantly. While the weak and broadband emission spectrum of the neat dye solution at the high pump energy of 28.1 mJ/pulse exhibits the spontaneous emission of RhB dye with the central wavelength 598 nm, the intensive and narrowband emission of the sample composed of ZnS:Mn QDs and RhB dye implies the occurrence of random lasing action with nonresonant feedback [29,30]. It is because light multi-scatters by ZnS:Mn QDs dispersed in the gain medium. According to the RL theory with nonresonant feedback, light multi-scattering inside the random amplifying medium increases the path length and dwell time of the emitted light. As a result, light gains more amplification before it leaves the medium. When the gain length approaches the average path length of the emitted light, the lasing condition is full-filled and the emission intensity starts to increase quickly for the wavelengths near the maximum of the gain line-shape. This phenomenon is accompanied by a drastic reduction of the emission linewidth. The gain length of the emitted light reduces by increasing the pump energy, while the average path length increases in the presence of scattering particles [50]. Therefore, the lasing condition cannot be full-filled in the absence of scattering particles even in high enough pump energies. Due to the lack of resonant conditions, the obtained

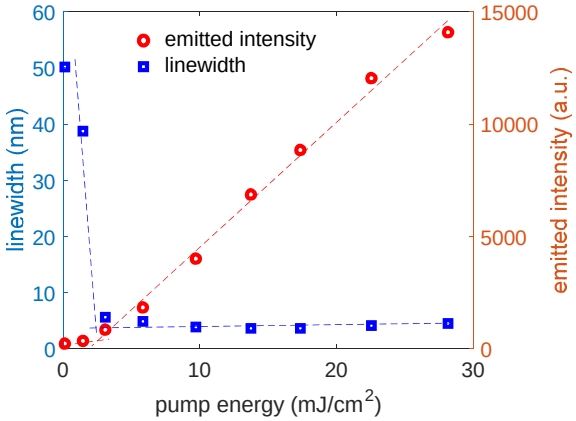

Fig. 4. Linewidth of the emission peak and the corresponding maximum emitted intensity in arbitrary units versus the pump energy for the sample composed of 10.44 mM RhB dye and 35 mg mL^{-1} ZnS:Mn QDs.

emission light with lasing characteristics is called the RL emission with nonresonant feedback. This is the reason explaining the more intensive and narrowband emission of the sample composed of 35 mg mL^{-1} ZnS:Mn QDs and 10.44 mM RhB dye compared with that of the neat dye solution, depicted in Fig. 3.

To measure the minimum pump energy required for the onset of random lasing emission from the sample composed of 35 mg mL^{-1} ZnS:Mn QDs and 10.44 mM RhB dye, one needs to plot the curve of maximum emitted intensity versus the pump energy. By measuring the maximum emitted intensity at each value of the pump energy, we obtain the data marked with circles in the curve depicted in Fig. 4. The main feature in Fig. 4 is that the maximum emitted intensity evolves nonlinearly with the pump energy. This is also true for the variation of the emission linewidth versus the pump energy, shown separately in Fig. 4. In such a case, well-known as the threshold behavior, the emission intensity (linewidth) increases (decreases) monotonically by increasing the pump energy. When the pump energy approaches a special value, the increasing intensity

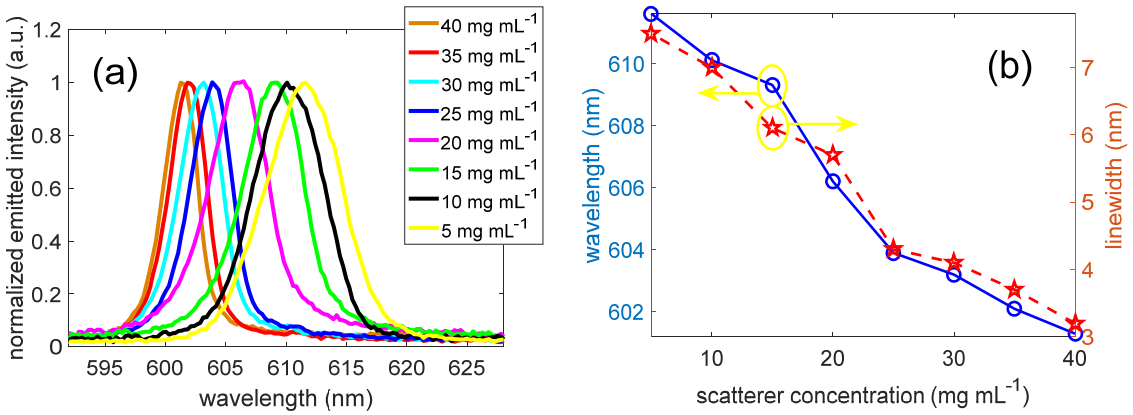

Fig. 5. (a) Normalized emission spectra of the samples composed of 10.44 mM RhB dye with different concentrations of ZnS:Mn QDs, (b) blue-shift of the emission wavelength and linewidth narrowing by increasing the concentration of ZnS:Mn QDs. The pump energy is 17.3 mJ/pulse.

(decreasing linewidth) continues to build up (down) very quickly. By further increasing the pump energy, the maximum emitted intensity increases rapidly but the emission linewidth remains nearly constant. One can observe in Fig. 4 that the threshold pump energy can be estimated approximately as 2.8 mJ/cm^2 from both curves illustrating the variations of the maximum emitted intensity and linewidth as a function of the pump energy. According to the RL theory, the increased gain balances with the losses at the threshold pump energy and the random lasing oscillation triggers. For RLs, the value of the threshold pump energy depends on the conditions providing the balance of gain and loss. In a random amplifying medium, successive multiple scattering events increases the path length of light and provides more optical amplification. Therefore, regarding the discussions in this paragraph and the previous paragraph, the emission intensity is increased and the RL threshold is decreased by increasing the scattering strength of light. It will be studied in the next paragraphs.

One way to validate the role of ZnS:Mn QDs as the scattering element in the fabricated RL, is to change their concentration and investigate the related spectral changes of the corresponding RL emission spectrum. In an effort to study the RL spectral dependences on the scatterer concentration, we repeat the previous procedures for the samples composed of 10.44 mM RhB dye and different concentrations of ZnS:Mn QDs such as 5 mg mL^{-1}, 10 mg mL^{-1}, 15 mg mL^{-1}, 20 mg mL^{-1}, 25 mg mL^{-1}, 30 mg mL^{-1} and 40 mg mL^{-1}. Obtained results reveal that the emission wavelength, linewidth and the RL threshold vary noticeably by changing the concentration of ZnS:Mn QDs as the light scatterers. Figure 5(a) shows the normalized emission spectra of the samples composed of 10.44 mM RhB dye and different concentrations of ZnS:Mn QDs at the same pump energy 17.3 mJ/pulse. It is clearly seen that the emission wavelength blue shifts by increasing the scatterer concentration from 5 mg mL^{-1} to 40 mg mL^{-1}. Also, one may notice the linewidth narrowing by the increase of the scatterer concentration. As it is confirmed in Fig. 5(b), the emission linewidth reduces from 7.5 nm to 3.2 nm, by increasing the scattering concentration from 5 mg mL^{-1} to 40 mg mL^{-1}. The emission wavelength also reduces from 611.6 nm for the scattering concentration of 5 mg mL^{-1} to 601.3 nm for the scattering concentration of 40 mg mL^{-1}, exhibiting an overall blue shift of 10.3 nm by increasing the concentration of the scatterers.

Considering the nonresonant nature of the feedback mechanism in the obtained random lasing emission, the lasing wavelength follows the spectral variations of the gain lineshape as a function of the scatterer concentration. To gain an insight into the spectral blue-shift of the random lasing emission, we use the following relation for calculating the emission intensity of RhB dye molecules in the presence of the scatterer nanoparticles when the pump energy is below the RL threshold [47]:

$$I(\lambda, l_t) = I_0(\lambda)\exp(-\alpha(\lambda)\cdot l_t) \quad (2)$$

Where $I_0(\lambda)$ is the emission intensity of RhB dye molecules in the absence of the scatterer nanoparticles (photoluminescence spectrum). Also $\alpha(\lambda)$ is the absorption coefficient which is obtained from the measurement of absorption spectrum of RhB dye solution via the following relation:

$$\alpha(\lambda) = A(L)/L \quad (3)$$

where A(λ) is the absorption spectrum of dye solution and L is the sample thickness along the direction of incident beam applied for the measurement of A(λ). Furthermore, the transport mean free path of light (l_t) can be calculated from the following approximate relation:

$$l_t = \frac{1}{\rho\sigma_{scat}} \quad (4)$$

where the σ_{sca} and ρ denote the scattering cross section and the volume density of ZnS-Mn QDs, respectively. We use the Mie scattering theory for calculating the scattering cross section of ZnS-Mn QDs. With some mathematical calculations, we obtain l_t values for solutions with different concentrations of GQDs and give the corresponding results in Table. 1. One can see that l_t values decrease with increase of ZnS-Mn QDs concentration. In addition, we measure the photoluminescence and absorption spectra of RhB dye, in order to obtain the wavelength dependences of $I_0(\lambda)$ and $\alpha(\lambda)$. The photoluminescence spectrum of RhB dye

Table 1. Values of the light transport mean free path (l_t), RL threshold, wavelength and linewidth (FWHM) corresponding to the samples consisting 10.44 mM RhB dye and different concentrations of ZnS:Mn QDs. The pump energy is 13.7 mJ/cm^2.

Scatterer concentration (mg mL^{-1})	Light transport mean free path (μm)	RL Threshold (mJ/cm^2)	Wavelength (nm)	Linewidth (FWHM) (nm)
5	6.0236×10^3	12.2	611.6	7.5
10	3.0118×10^3	9.3	610.1	7.0
15	2.0073×10^3	6.2	609.3	6.1
20	1.5056×10^3	5.1	606.2	5.7
25	1.2043×10^3	4.0	603.9	4.3
30	1.0036×10^3	3.5	603.2	4.1
35	8.6024×10^2	2.8	602.1	3.7
40	7.5274×10^2	2.3	601.3	3.2

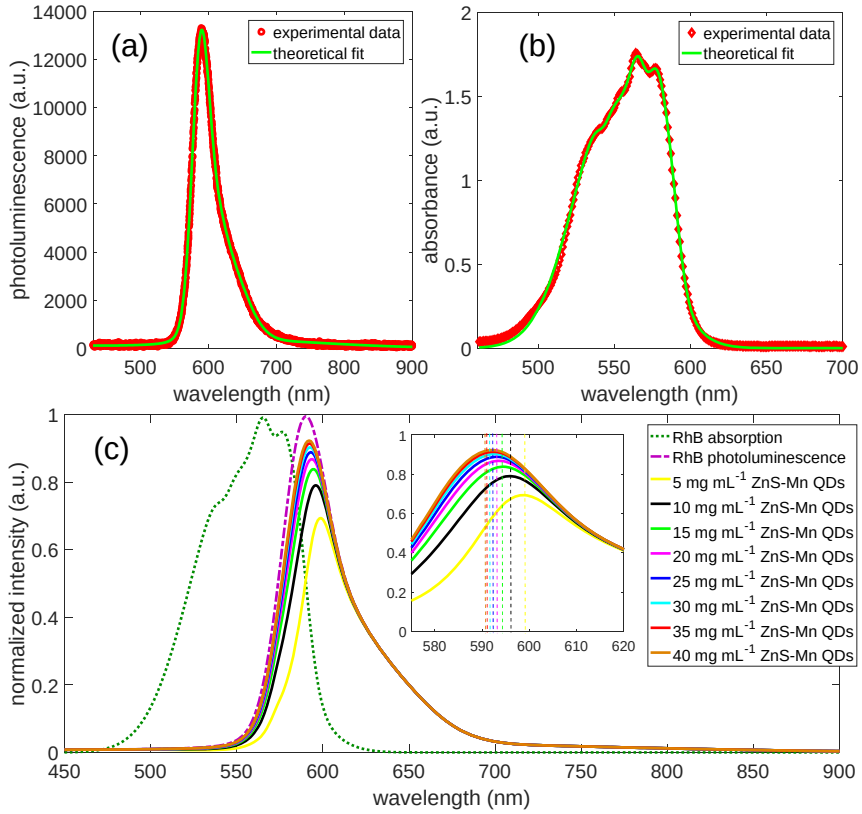

Fig. 6. (a) Normalized photoluminescence spectrum of RhB dye, (b) Normalized absorption spectrum of RhB dye, (c) Calculated fluorescence spectra of RhB dye in the presence of ZnS:Mn QDs inside the gain medium as the light scatterers. The inset displays the enlarged fluorescence spectra of RhB dye and illustrates the spectral blue-shift of the fluorescence spectrum by the increase of the scatterer concentration. The vertical dashed lines indicate the spectral positions of the maximum emitted intensity corresponding to each curve.

with the central wavelength 589.5 nm is obtained under excitation by a continuous-wave Nd-YAG laser with wavelength 532 nm. The normalized photoluminescence and absorption spectra of RhB dye are depicted in figures 6 (a) and (b), respectively. The absorption spectrum of RhB dye covers a relatively wide spectral range from 465 nm to 615 nm and exhibits a peak at 564 nm. Since the number of the experimental data corresponding to the photoluminescence and absorption spectra of RhB dye are not the same, to calculate $I(\lambda,l_t)$, we need to regenerate the $I_0(\lambda)$ and $\sigma_{abs}(\lambda)$ spectra. For this purpose, we sum five Gaussian functions to fit the experimental curves, properly. As it is shown by the solid lines in figures 6 (a) and (b), the theoretical fitting curves can regenerate the experimental data. Hence, we use the theoretical fitting equations as the $I_0(\lambda)$ and $\sigma_{abs}(\lambda)$ spectra and calculate the $I(\lambda,l_t)$ spectra from Eq. (2) for each value of l_t. The results corresponding to different values of l_t are depicted in Fig. 6 (c), illustrating a 8 nm blue-shift of the gain line-shape from the wavelength of 599 nm to 591 nm, by an increase in the scatterer concentration. As a result, the lasing wavelength exhibits a spectral blue-shift, when the scatterer concentration increases. Another noticeable point in Fig. 6 (c) is the red-shift of the gain lineshape in the presence of the scatterer nanoparticles compared to the photoluminescence spectrum $I_0(\lambda)$. This phenomenon can be explained based on the reabsorption and reemission of light by the dye molecules [51]. The spectral overlap of RhB absorption and emission spectra

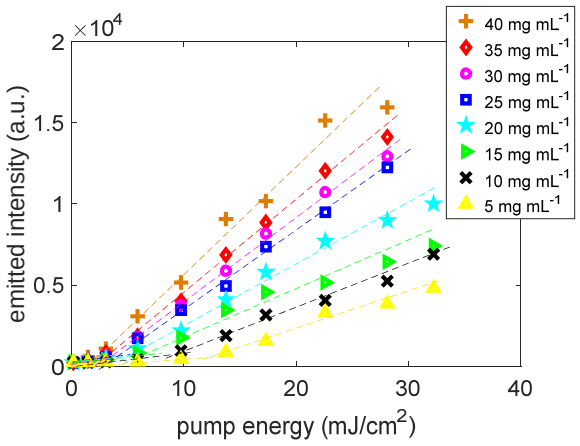

Fig. 7. Plots of the maximum emitted intensity in arbitrary units versus the pump energy for the samples composed of 10.44 mM RhB dye and different concentrations of ZnS:Mn QDs.

is clearly observed in Fig. 6 (c), implying the reabsorption of the emitted light photons and then reemission at the longer wavelengths. Since the optical path length and dwell time of light photons increase in the disordered amplifying medium, the reabsorption and reemission of light occurs more. This phenomenon results in the red-shift of the emission wavelength compared to the situation in which no scatterers are present in the gain medium.

According to Eq. (4), the scattering mean free path (l_t) reduces by the increase of σ_{sca} and ρ. With a decrease in l_t, the light paths in the disordered amplifying medium increase and the optical feedback provided by the scattering, enhances. Since light gains more amplification, it is then expected that the random lasing threshold decreases by the increase of the scatterer concentration. This theoretical explanation is confirmed in Fig. 7 in which the threshold behaviors of the eight samples containing the same concentration of 10.44 mM RhB dye but different concentrations of ZnS:Mn QDs are compared with each other. The dashed lines are curve fitting to the experimental data. It is clearly seen that the RL threshold decreases from 12.2 mJ/cm^2 to 2.3 mJ/cm^2, when the concentration of ZnS:Mn QDs increases from 5 mg mL^{-1} to 40 mg mL^{-1}. Also, the slope efficiency increases when the scatterer concentration increases. The detailed information on the values of l_t, RL threshold, the emission wavelength and the emission linewidth (FWHM) corresponding to the prepared samples are presented in table 1.

The obtained results in this paper show that ZnS:Mn QDs can act potentially well as the scattering medium in a dye solution-based RL. Since, to our knowledge, there are no reported experiments on the RLs fabricated based on ZnS:Mn nanocrystals, we hope that this work can pave the way for further experimental investigations on the RLs fabricated based on ZnS QDs used as the gain or scattering medium. Due to the bright yellow photoluminescence, lower toxicity and better efficiency of ZnS:Mn QDs compared with CdSe and CdS QDs, these new RLs are more promising for sensing, bio-labeling and bio-imaging applications. In addition, changing the concentration of Mn^{2+} ions is expected to optimize the corresponding RL emission properties and make the RL controllable, by changing the optical and electronic properties of ZnS:Mn QDs. Furthermore, the tunability of the lasing emission by changing the concentration of the scatterers may be advantageous in practical applications for controlling and engineering the emission wavelength and random lasing threshold. By suggesting these points, we hope that this work can push ahead the researches on QDs based RLs.

4. Conclusion

To conclude, we report on the fabrication of a dye-based RL with nonresonant feedback using ZnS:Mn QDs as the scattering medium and RhB dye as the gain medium. We observe that the output emission intensity increases and the emission linewidth decreases, by an increase in the pump energy. Furthermore, we observe a blue-shift of approximately 10.3 nm, a decrease in the emission linewidth by 4.3 nm and a decrease in the RL threshold by 9.9 mJ/cm^2, when the scatterer concentration increases by 35 mg mL^{-1}. This approach can be applied for controlling and engineering the emission wavelength and random lasing threshold for desired applications.

References

1. N M Lawandy, R M Balachandran, A S L Gomes and E Sauvain, "*Laser Action In Strongly Scattering Media*," *Nature*, Vol. **368** (1994) 436.
2. H Cao, Y G Zhao, S T Ho, E W Seelig, Q H Wang and R P H Chang, "*Random Laser Action In Semiconductor Powder*," *Phys. Rev. Lett*. Vol. **82** (1998) 2278.
3. L Yang, G Feng, J Yi, K Yao, G Deng and S Zhou, "*Effective random laser action in Rhodamine 6G solution with Al nanoparticles*," *Appl. Opt.* Vol. **50** (2011) 1816.
4. S Xiao, T Li, D Huang, M Xu, H Hu, S Liu, C Wang and T Yi, "*Random laser action from ceramic doped polymer films*," *J. Modern Opt*. Vol. **64** (2017) 1289.

5. G D Dice, S Mujumdar and A Y Elezzabi, "*Plasmonically enhanced diffusive and subdiffusive metal nanoparticle-dye random laser*," *Appl. Phys. Lett*. Vol. **86** (2005) 131105.
6. S Ning, Z Wu, H Dong, L Ma, B Jiao, Le Ding, Li Ding and F Zhang, "*The Enhanced Random Lasing From Dye Doped Polymer Films With Different-Sized Silver Nanoparticles*," *Organic Electronics*, Vol. **30** (2016) 165.
7. Z Shang, Z Tao and L Deng, "*Random lasing assisted by $CuSO_4$ and Au nanoparticles in random gain systems*," *Opt. Mater. Exp*. Vol. **7** (2017) 1848.
8. E Heydari, I P Santos, L M L Marzán and J Stumpe, "*Nanoplasmonically-engineered random lasing in organic semiconductor thin films*," *Nanoscale Hariz*. Vol. **2** (2017) 261.
9. B R Anderson, R Gunawidjaja and H Eilers, "*Low-threshold and narrow linewidth diffusive random lasing in rhodamine 6G dye-doped polyurethane with dispersed ZrO_2 nanoparticles*," *J. Opt. Soc. Am*. B Vol. **31** (2014) 2363.
10. E Jimenez-Villar, V Mestre, P C de Oliveira, W M Faustino, D S Silva and G F de Sá, "*TiO2@Silica nanoparticles in a random laser: Strong relationship of silica shell thickness on scattering medium properties and random laser performance*," *Appl. Phys. Lett*. Vol. **104** (2014) 081909.
11. L Ye, J Lu, C Lv, Y Feng, C Zhao, Z Wang and Y Cui, "*Random lasing action in magnetic nanoparticles doped dye solutions*," *Opt. Commun*. Vol. **340** (2015) 151.
12. L A Moura, P I R Pincheira, L J Q Maia, A S L Gomes and C B de Araújo, "*Two-color random laser based on a Nd^{3+} doped crystalline powder*," *J. Luminescence*, Vol. **181** (2017) 44.
13. R B Silva, A F Silva, A M B Silva and C B de Araújo, "*Bichromatic random laser from a powder of rhodamine-doped sub-micrometer silica particles*," *J. Appl. Phys*. Vol. **115** (2014) 043515.
14. S G Revilla, M Zayat, R Balda, M A Saleh, D Levy and J Fernández, "*Low threshold random lasing in dye-doped silica nano powders*," *Opt. Exp*. Vol. **17** (2009) 13202.
15. B H Hokr, J N Bixler, M T cone, J D Mason, H T Beier, G D Noojin, G I Petrov, L A Golovan, R J Thomas, B A Rockwell and V V Yakovlev, "*Bright emission from a random Raman laser*," *Nat. Comm*. Vol. **5** (2014) 1.
16. A Consoli and C López, "*Lasing optical cavities based on macroscopic scattering elements*," *Scientific Reports*, Vol. **7** (2017) 40141.
17. T Zhai, X Zhang, Z Pang, X Su, H Liu, S Feng and L Wang, "*Random laser based on waveguided plasmonic gain channels*," *Nano Lett*. Vol. **11** (2011) 4295.
18. J Yin, G Feng, S Zhou, Ho Zhang, S Wang and H Zhang, "*The effect of the size of Au nanorods on random laser action in a disordered media of ethylene glycol doped with Rh6G dye*," *Proc. SPIE Nanophotonics VI*, Vol. **9884** (2016) 988426.
19. T Zhai, J Chen, L Chen, J Wang, L Wang, D Liu, S Li, H Liu and X Zhang, "*A plasmonic random laser tunable through stretching silver nanowires embedded in a flexible substrate*," *Nanoscale*, Vol. **7** (2015) 2235.
20. Q Chang, X Shi, X Liu, J Tong, D Liu and Z Wang, "*Broadband plasmonic silver nanoflowers for high-performance random lasing covering visible region*," *Nanophotonics*, Vol. **6** (2017) 1151.
21. A Yadav, L Zhong, J Sun, L Jiang, G J Cheng and L Chi, "*Tunable random lasing behavior in plasmonic nanostructures*," *Nano Convergence*, Vol. **4** (2017) 1.
22. A G Ardakani, P Rafieipour, "*Using ZnO nanosheets grown by electrodeposition in random lasers as scattering centers: the effects of sheet size and presence of mode competition*," *J. Opt. Soc. Am*. B. Vol. **35** (2018) 1708.
23. H Zhang, G Feng, H Zhang, C Yang, J Yin and S Zhou, "*Random laser based on Rhodamine 6G (Rh6G) doped poly(methyl methacrylate) (PMMA) films coating on ZnO nanorods synthesized by hydrothermal oxidation*," *Results in Physics*, Vol. **7** (2017) 2968.
24. Y C Chen, C S Wang, T Y Chang, T Y Lin, H M Lin and Y F Chen, "*Ultraviolet and visible random lasers assisted by diatom frustules*," *Opt. Exp*. Vol. **23** (2015) 16224.
25. P K Roy, G Haider, H Lin, Y M Liao, C H Lu, K H Chen, L C Chen, W H Shih, C T Liang and Y F Chen, "*Multicolor ultralow-threshold random laser assisted by vertical-graphene network*," *Adv. Opt. Mater*. Vol. **6** (2018) 1800382.
26. S H Cheng, Y C Yeh, M L Lu, C W Chen and Y F Chen, "*Enhancement of laser action in ZnO nanorods assisted by surface Plasmon resonance of reduced graphene oxide nanoflakes*," *Opt. Exp.* Vol. **20** (2012) 799.
27. W C Liao, Y M Liao, C T Su, P Perumal, S Y Lin, W J Lin, C H Chang, H I Lin, G Haider, C Y Chang, S W Chang, C Y Tsai, T C Lu, T Y Lin and Y F Chen, "*Plasmonic carbon-dot-decorated nanostructured semiconductors for efficient and tunable random laser action*," *ACS Appl. Nano Mater*. Vol. **1** (2018) 152.
28. D Zhang, G Kostovski, C Karnutsch and A Mitchell, "*Random lasing from dye doped polymer within biological source scatters: The pomponia imperatorial cicada wing random nanostructures*," *Organic Electron*. Vol. **13** (2012) 2342.
29. H Cao, "*Lasing in random media*," *Waves Random Media*. Vol. **13** (2003) R1-R39.
30. H Cao, "*Random lasers: development, features and applications*," *Opt. and photonics news*, Vol. **16** (2005) 24.
31. F Luan, B Gu, A S. L Gomes, K Yong, S Wen and P N Prasad, "*Lasing in nano-composite random media*," *Nano Today*, Vol. **10** (2015) 168.
32. D V Churkin, S Sugavanam, I D Vatnik, Z Wang, E V Podivilov, S A Babin, Y Rao and S K Turitsyn, "*Recent advances in fundamentals and applications of random fiber lasers*," *Adv. Opt. Photon*. Vol. **7**

(2015) 516.
33. X Du, H Zhang, H Xiao, P Ma, X Wang, P Zhou and Z Liu, "*High-power random distributed feedback fiber laser: From science to application*," *Ann. Phys* (Berlin), Vol. **528** (2016) 649.
34. S F Yu, "*Electrically pumped random lasers*," *J. Phys. D: Appl. Phys*. Vol. **48** (2015) 483001.
35. Y Chen, J Herrnsdorf, B Guilhabert, Y Zhang, I M Watson, E Gu, N Laurand and M D Dawson, "*colloidal quantum dot random laser*," *Opt. Exp*. Vol. **19** (2011) 2996.
36. Y Yung-Chi, Z P Yang, J M Hwang, H C Su, J Y Haung, T N Lin, J L Shen, M H Lee, M T Tsai and Y J Lee, "*Coherent and polarized random laser emissions from colloidal CdSe/ZnS quantum dots plasmonically coupled to ellipsoidal Ag nanoparticles*," *Adv. Opt. Mat*. Vol. **5** (2017) 1600746.
37. M Cao, Y Zhang, X Song, Y Che, H Zhang, H Dai, G Zhang and J Yao, "*Random lasing in a colloidal quantum dot-doped disordered polymer*," *Opt. Exp*. Vol. **24** (2016) 9325.
38. C Gollner, J Ziegler, L Protesescu, D N Dirin, R T Lechner, G F Popovski, M Sytnyk, S Yakunin, S Rotter, A A Y Amin, C Vidal, C Hrelescu, T A Klar, M Kovalenko and W Heiss, "*Random lasing with systematic threshold behavior in films of CdSe/CdS core/thick-shell colloidal quantum dots*," *ACS Nano*, Vol. **9** (2015) 9792.
39. A K Augustine, P Radhakrishnan, V P N Nampoori and M Kailasnath, "*Enhanced random lasing from a colloidal CdSe quantum dot-Rh6G system*," *Laser Phys. Lett*. Vol. **12** (2015) 0250061.
40. L W Li, "*Random lasing characteristics in dye-doped semiconductor CdS nanoparticles*," *Laser Phys. Lett*. Vol. **13** (2016) 015206.
J Yi, G Feng, C Yang, H Zhang, K Yao and S Zhou, "*2.18 μm random laser action based on Cr^{2+}:ZnSe nanocrystalline particles*," *Opt. Commun*. Vol. **309** (2013) 170.
42. T Takahashi, T Nakamura and S Adachi, "*Blue-light-emitting ZnSe random laser*," *Opt. Lett.* Vol. **34** (2015) 3923.
43. X Yang, G Feng, K Yao, J Yi, H Zhang and S Zhou, "*Random lasing of microporous surface of Cr^{2+}:ZnSe crystal induced by femtosecond laser*," *AIP Adv*. Vol. **5** (2015) 067160.
44. H Labiadh, T B Chaabane, D Piatkowski, S Mackowski, J Lalevée, J Ghanbaja, F Aldeek and R Schneider, "*Aqueous route to color-tunable Mn-doped ZnS quantum dots*," *Mater. Chem. Phys*. Vol. **140** (2013) 674.
45. X Ma, J Song and Z Yu, "*The light emission properties of ZnS:Mn nanoparticles*," Thin Solid Films, Vol. **519** (2011) 5043.
46. Z Rui, L Yingbo and S Shuqing, "*Synthesis and characterization of high-quality colloidal Mn^{2+}-doped ZnS nanoparticles*," *Opt. Mater*. Vol. **34** (2012) 1788.
47. F Shuzhen, Z Xingyu, W Qingpu, Z Chen, W Zhengping and L Ruijun, "*Inflection point of the spectral shifts of the random lasing in dye solution with TiO2 nanoscatterers*," *J. Phys. D: Appl. Phys*. Vol. **42** (2009) 015105.
48. J Kitur, G Zhu, M Bahoura and M A Noginov, "*Dependence of the random laser behavior on the concentrations of dye and scatterers*," *J. Opt.* Vol. **12** (2010) 024009.
49. B H Zhang, F Y Wu, Y M Wu and X S Zhan, "*Fluorescent method for the determination of sulfide anion with ZnS:Mn quantum dots*," *J. Fluorescence*, Vol. **20** (2010) 243.
50. A S Wiresma, A Lagendijk, "*Lasing diffusion with gain and random lasers*", *Phys. Rev*. E Vol. **54** (1996) 4256.
51. A L Moura, R B Silva, C T Dominguez, É Pecoraro, A S L Gomes and C B de Araújo, "*Single bead near-infrared random laser based on silica-gel infiltrated with Rhodamine 640*," *J. Appl. Phys*. Vol. **123**, (2018) 133104.